



ELSEVIER

Solar Energy Materials & Solar Cells 63 (2000) 61–68

www.elsevier.com/locate/solmat

Solar Energy Materials
& Solar Cells

Comparison of photovoltaic devices containing various blends of polymer and fullerene derivatives

T. Fromherz^{a,*}, F. Padinger^a, D. Gebeyehu^b, C. Brabec^c,
J.C. Hummelen^d, N.S. Sariciftci^b

^aQuantum Solar Energy Linz (QSEL), A-4010 Linz, Austria

^bInstitute for Physical Chemistry, Johannes Kepler University Linz, A-4040 Linz, Austria

^cChristian Doppler Laboratory for Plastic Solar Cells, Physical Chemistry, Johannes Kepler University, A-4040 Linz, Austria

^dStratingh Institute and Materials Science Center, University of Groningen, 9747 AG Groningen, Netherlands

Received 10 February 1999; received in revised form 17 May 1999; accepted 28 May 1999

Abstract

Large area photovoltaic devices based on an interpenetrating network of donor and acceptor molecules have been fabricated showing power conversion efficiencies up to 1.5% under monochromatic illumination at 500 nm. Devices containing blends of solubilized poly (para-phenylene vinylene), (PPV) or poly thiophene derivatives as donors with various fullerene derivatives as acceptors are compared. It is shown that among the various combinations of materials both the open-circuit voltage and the short-circuit current are maximal for a blend of PPV and a highly soluble methano fullerene. For a further increase of the efficiency of these devices, a reduction of the thickness of the active layer is suggested. © 2000 Elsevier Science B.V. All rights reserved.

Keywords: Solar cells; Poly (para phenylene vinylene) and derivatives; Poly thiophene and derivatives; Fullerenes and derivatives; Bulk heterojunction

1. Introduction

The demand for inexpensive, renewable energy sources is driving new approaches to the production of low-cost photovoltaic devices. In the last couple of years, a large

* Corresponding author.

amount of effort has been put in the development of solar cells based on organic molecules (see for example [1]) and conjugated polymers ([2,3] and references therein). Especially polymer-based solar cells would offer considerable advantages for the fabrication, like low-cost roll-to-roll production of large area, flexible solar cells. Because of these advantages, the development of polymer solar cells is supposed to have a major impact, even if the efficiencies of these polymer photovoltaic devices up to now are noticeably smaller than the efficiencies achieved in inorganic (for example Si) solar cells.

For the generation of electrical power by absorption of photons it is necessary to spatially separate the electron-hole (e-h) pair generated in the primary absorption process before recombination processes can take place. In conjugated polymers, the stabilization of the photoexcited e-h pair can be achieved by blending the polymer with an acceptor molecule having an electron affinity that is larger than the electron affinity of the polymer but still smaller than its ionization potential. Under these conditions, photoinduced electron transfer from the conjugated polymer to the acceptor molecule is energetically favourable.

In our work, this alignment of the energy levels is realized by blending solubilized poly phenylene vinylene or poly thiophene derivatives (acting as photoexcited electron donors) with derivatives of C_{60} (electron acceptor). It has been shown that in these systems the transfer of the photoexcited electrons onto the fullerenes occurs within approximately 200 fs after the excitation [4]. Since all other known competing relaxation processes in conjugated polymers occur on time scales that are orders of magnitudes larger than 200 fs, this ultra fast charge transfer must have a quantum efficiency of approximately 1, i.e. nearly all electrons excited by the absorption of a band-gap photon are transferred to C_{60} . In addition, the relaxation of the charge separated excited state takes place on a μ s-time scale at room temperature [4], allowing the generation of high concentrations of non-equilibrium electrons and holes.

By sandwiching the blend of conjugated polymers and C_{60} between electrodes that have different work functions $q\Phi_m$ (for example ITO (indium tin oxide, $q\Phi_m = 4.7$ eV) and Al ($q\Phi_m = 4.3$ eV)) an electrical field is established across the polymer layer. For acceptor concentrations greater than the percolation threshold of 17 mol% [5], the non-equilibrium carriers generated by the incident light are separated and driven towards their respective contacts under this electric field and a current is delivered to an electrical circuit connected to the electrodes. However, the mobilities of electrons and holes are rather small in the polymer blends used in this work (in the order of 10^{-4} cm²/Vs), limiting the efficiency of the photovoltaic cells. In the following we compare the I - V characteristics of devices made from PPV and P3OT blended with various C_{60} derivatives. In addition, it is shown that by decreasing the device thickness to an optimum value, the efficiency can be increased significantly.

2. Experimental procedure

The photovoltaic devices have been cast from solutions of poly [2-methoxy, 5-(3',7'-dimethyl-octyloxy)]-p-phenylene vinylene (MDMO-PPV) in toluene or poly

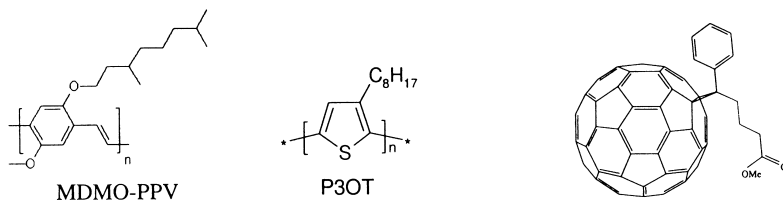


Fig. 1. Molecular structure of the polymers and PCBM monoadduct used in this work.

(3-octylthiophene) (P3OT) in xylene at room conditions in a laminar flow box. These polymers act as electron donors when blended with solutions of the acceptor molecules C₆₀ as well as mono- and multiadducts of the solubilized C₆₀ derivative [6,6]-Phenyl C₆₁-butyric acid methyl ester (PCBM). The PCBM multiadduct is a mixture of mono, bis and tris adducts on the fullerene. The chemical structure of the compounds is shown in Fig. 1. The enhanced solubility of PCBM compared to C₆₀ allows a high fullerene-conjugated polymer ratio and, therefore, strongly supports the formation of an interpenetrating network of donor and acceptor molecules (donor–acceptor bulk heterojunction). Consequently, the photovoltaic devices investigated in this paper were cast from solutions with weight ratios between PCBM and the conjugated polymer of 3 : 1, whereas for the devices made with C₆₀ as acceptor, the respective weight ratios were 1 : 1. The thickness of the polymer: C₆₀ layers is in the range of 100–200 nm. As a substrate, a flexible PET foil covered with ITO ($R_s = 55 \Omega/\square$) was used. For contact improvement, the ITO was coated with a thin layer of poly(ethylene dioxythiophene) (PEDOT). The top electrode was formed by vacuum evaporation of $1 \times 4 \text{ cm}^2$ Al stripes.

3. Results and discussion

In Fig. 2, the current–voltage (I – V) characteristics under white light ($6 \text{ mW}/\text{cm}^2$, Fig. 2a) and in the dark (Fig. 2b) of photovoltaic devices made from a blend of MDMO–PPV with different C₆₀ derivatives are compared (because of the logarithmic scale of the current axis, the absolute value of the current is plotted against the voltage in Fig. 2). It is clearly shown that the highest (lowest) short-circuit current is observed when PCBM monoadduct (PCBM multiadduct) is used as electron acceptor ($|I_{sc}| = 1$ and 0.20 mA , respectively). The open-circuit potentials V_{oc} of the three devices shown in Fig. 2a are around $V_{oc} = 0.72 \text{ V}$. It is worth noting that the measured open-circuit voltage is significantly higher than one would expect from a simple model describing the device as a metal–insulator–metal (MIM) diode. In such a model, the difference of the work functions of the electrode materials defines the upper limit of the open-circuit voltage. Although the work function of ITO is a poorly defined quantity (values ranging from 5.5 [6] to 4.1 eV [7] are reported in literature), recent estimates seem to converge into the range between 4.4 – 4.7 eV [8,9]. Using these values for the ITO work function and 4.3 eV for the Al work function, one would expect the

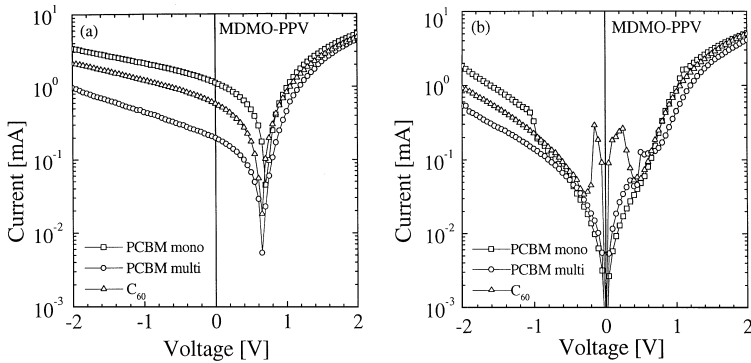


Fig. 2. Current–voltage characteristics of devices (4 cm^2) made from MDMO–PPV blended with different fullerene derivatives measured under illumination (a) and in the dark (b): PCBM monoadduct (squares), PCBM multiadduct (circles), and C_{60} (triangles). Because of the logarithmic scale, the absolute value of the current is plotted.

open-circuit voltage of an ITO/polymer: C_{60} Al device to be not larger than 0.4 V. Experimentally, however, a open-circuit voltage of 0.72 V is observed. Up to now, the origin of the high open-circuit voltage is not fully understood, it might be due to a formation of a space charge layer at the interface between the polymer and one or both of the electrodes [10]. From our experiments, it is not clear yet whether the space charge is built up at the ITO or the Al electrode. Interestingly, in the I – V curves of these devices measured in the dark, structures are observed at an applied voltage equal to the work function differences (0.4–0.5 eV, see Fig. 2b). In addition, negative differential resistance is observed in the I – V curve measured in the dark of the device with C_{60} . Similar anomalies were observed in the I – V characteristics of organic multi-layer light emitting diodes [11].

In Fig. 3, the I – V curves for devices with P3OT as electron donating polymer blended with the same C_{60} derivatives as used for the devices shown in Fig. 2 are plotted. In the case of P3OT, the highest short-circuit current was obtained with C_{60} as acceptor molecule ($|I_{sc}| = 0.90\text{ mA}$). In these samples, a significant dependence of V_{oc} on the acceptor molecule was observed, the following values were measured samples (see Fig. 3a): 0.5 V for PCBM multiadduct, 0.55 V for C_{60} and 0.6 V for PCBM monoadduct. Again, from the simple MIM model, one would expect an open-circuit voltage independent of the acceptor molecule.

From a measurement of the short-circuit current density (i_{sc}) the ratio η_c of the number of the incident photons to the number of the electrons delivered to an external circuit (IPCE) is calculated according to

$$\eta_c = \frac{E_{ph}(\lambda) i_{sc}}{P_{in} e}, \quad (1)$$

where λ , E_{ph} and P_{in} denote the wavelength, the photon energy and the intensity of the incident radiation and e is the elementary charge. For a typical photovoltaic device

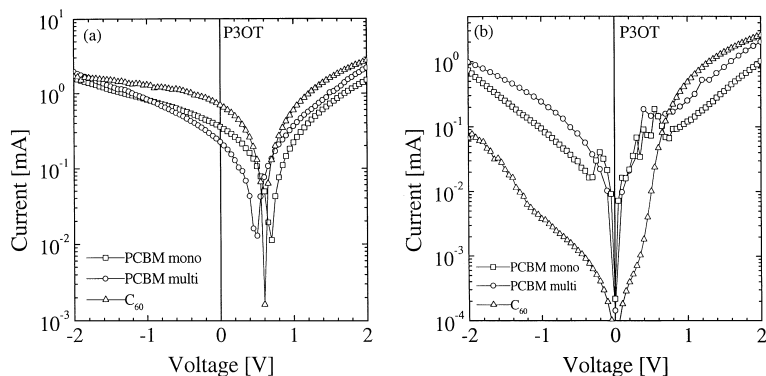


Fig. 3. Same as Fig. 2 for blends with P3OT and different fullerene derivatives.

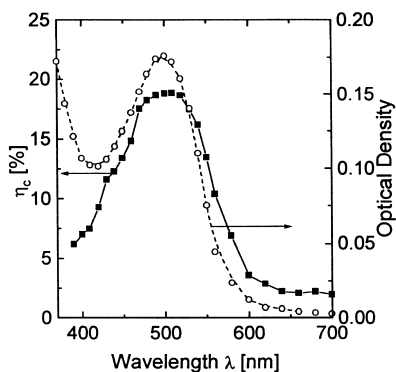


Fig. 4. Ratio of converted electrons to incident photons (η_c , full symbols, left scale) optical density ($\alpha_{10}d$, open symbols, right scale) as a function of the wavelength of the incident radiation for a MDMO-PPV:PCBM monoadduct device. For all wavelengths, the excitation intensity was kept constant at $1 \text{ mW}/\text{cm}^2$.

containing a blend of MDMO-PPV and PCBM monoadduct as photoactive layer, η_c as a function of the wavelength in the range between 400 and 700 nm is shown in Fig. 4 (full symbols, left scale). The measurements were performed using a Xe arc lamp with a Czerny–Turner single pass monochromator as source. For each wavelength, the light intensity was kept constant at $1 \text{ mW}/\text{cm}^2$. Also shown in Fig. 4 is the optical density of the polymer layer (i.e. $\alpha_{10}d$, where α_{10} is the decadic absorption coefficient and d the thickness of layer) as a function of the wavelength as measured in transmission (open symbols, right scale). The absorption band in range between 450 and 600 nm is due to band-gap absorption of the polymer, whereas the increase of the absorption for wavelengths shorter than 400 nm is a superposition of the absorption of MDMO-PPV (370 nm) and PCBM (330 nm). Fig. 4 clearly shows that η_c closely follows the polymer band-gap absorption. The maximum value of η_c (17%) is observed at 500 nm. For this wavelength, the optical density as measured in

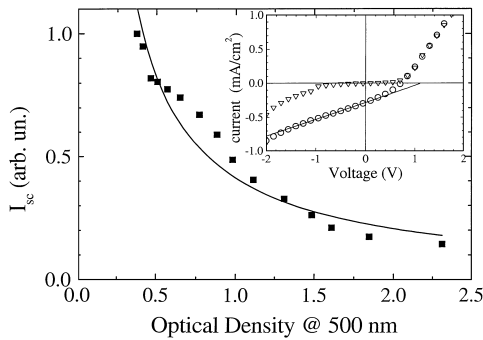


Fig. 5. Dependence of the normalized short-circuit current of MDMO–PPV:PCBM monoadduct devices on the optical density of the devices (squares). As discussed in the text, the data for I_{sc} were fitted to a reciprocal dependence on the optical density (full line). In the inset, a typical current–voltage characteristic of these devices is shown under illumination (circles) and in the dark (triangles). The full line in the inset is the result of a fit of the current–voltage characteristic in the range between 1.6 and 0.4 V to a linear dependence.

transmission is 0.18. Since in the photovoltaic device the incident light is reflected at the Al electrode, the absorption length in the device is twice its geometrical thickness. Neglecting the reflection from the surface of the device and also interference effects, at a wavelength of 500 nm the percentage of absorbed photons in this device can therefore be estimated by $1 - 10^{-0.18 \times 2} = 56\%$. Comparing this number to $\eta_c = 17\%$ shows that $< 50\%$ of the absorbed photons contribute to the short-circuit current.

In Fig. 5, the dependence of the short-circuit current on the optical density of a MDMO–PPV:PCBM blend layer is shown. Surprisingly, I_{sc} increases with decreasing layer thickness, showing that for thicker cells less photo-generated charges arrive at the electrodes but instead recombine in the polymer layer. A typical IV -curve of MDMO–PPV:PCBM diodes is plotted in the inset of Fig. 5. It shows that under illumination (circles in the inset), the absolute value of the photocurrent of the diode biased in back direction (negative voltages in the inset) increases *linear* with the absolute value of the applied voltage and thus of the electric field. The linear dependence of the photocurrent on the voltage is neither due to a shunt resistance – in this case, the same differential resistance would be observed in the IV curve measured in the dark (triangles in the inset of Fig. 5) – nor by a series resistance, since in forward direction (positive voltages in the inset of Fig. 5) the IV show a much smaller differential series resistance. For short-circuit conditions, the electric field in the polymer layer is established by the difference of the work functions of the electrode materials and consequently is inversely proportional to the polymer layer thickness. Together with the observed linear dependence of the photocurrent on the electric field, it follows that I_{sc} should be inversely proportional to the thickness of the MDMO–PPV:PCBM layer. Therefore, in Fig. 5 the data for I_{sc} are fitted to a $1/\alpha_{10}d$ dependence (shown by the solid line in Fig. 5). In spite of the strong simplifications assumed in the model, the data fit surprisingly well to it.

The optimal thickness (d_{opt}) of the polymer layer can be estimated by equating the ratio of absorbed to incident photons (for reflection geometry) to η_c .

$$1 - 10^{-\alpha_{10} \times 2d_{\text{opt}}} = \eta_c(d_{\text{opt}}). \quad (2)$$

In this case, all e–h pairs generated by the incident monochromatic radiation contribute to the short-circuit current. As a consequence of the assumed proportionality of the short-circuit current to $1/d$, the product of $\alpha_{10}d$ and η_c is independent of the thickness, as can be seen by multiplying Eq. (1) with $\alpha_{10}d$. Therefore, expanding the exponential function in Eq. (2) and multiplying by $\alpha_{10}d_{\text{opt}}$ yields

$$\alpha_{10}d_{\text{opt}} \approx \sqrt{\frac{\alpha_{10}d\eta_c(d)}{2\ln(10)}}, \quad (3)$$

where $\alpha_{10}d$ and η_c can be determined experimentally for devices with $d > d_{\text{opt}}$. The data shown in Fig. 4 were measured for a device made of the MDMO–PPV:PCBM blend (1:3) sandwiched between ITO and Al electrodes. For this type of device, at 500 nm one gets $\alpha_{10}d\eta_c = 0.03$, and therefore $\alpha_{10}d_{\text{opt}} \approx 0.08$ and $\eta_c(d_{\text{opt}}) \approx 0.31$. Up to now no detailed analysis of the optimal thickness has been performed for diodes made from a P3OT:C₆₀ blend.

Of course for applications, the power conversion efficiency η_e of the photovoltaic device is most important. It is related to the open-circuit voltage (V_{oc}), the filling factor (FF), i_{sc} , and P_{in} by

$$\eta_e = \frac{i_{\text{sc}} V_{\text{oc}} FF}{P_{\text{in}}} = \frac{\eta_c e V_{\text{oc}} FF}{E_{\text{ph}}}. \quad (4)$$

For the MDMO–PPV:PCBM samples, FF is typically in the range between 0.3 and 0.35 and $V_{\text{oc}} = 0.72$ (cf. Fig. 2). Therefore, for the sample shown in Fig. 4, at 500 nm the power conversion efficiency is 1.5%. As discussed above, for the same device architecture, the same morphology of the interpenetrating network, the same mobility of the charge carriers and an active layer with optimal thickness, η_c is expected to increase to 0.31. In addition, also the FF is expected to increase for thinner samples due to the reduction of the series resistance. Therefore, we estimate that with the polymer blend used in our samples the monochromatic power conversion efficiency can in principle be increased to approximately 3% by making devices with the optimized thickness.

For the PPV:PCBM blend used in the diodes presented in this paper, an absorption coefficient $\alpha_{10} = 2\text{--}3 \times 10^4 \text{ cm}^{-1}$ was measured, implying that the optimal thickness of these devices would be below 50 nm. For future large area production this is a high technological challenge. As an alternative, the use of polymer blends with increased electron and hole mobilities would relax the tight constraints on the optimal thickness and of course also increase the maximum achievable efficiency. We want to emphasize that in addition to raising the efficiency by increasing the absorption coefficient and/or increasing V_{oc} through the choice of appropriate donor and acceptor molecules [2], the optimization of the layer thickness offers another possibility to increase the conversion efficiency of a polymer solar cell.

4. Conclusions

For photovoltaic devices fabricated from several blends of MDMO–PPV and P3OT as donors and different fullerene derivatives (C_{60} , PCBM mono and multiadducts) as acceptors, the highest open-circuit voltage and short-circuit currents were obtained with a 1:3 (weight) blend of MDMO–PPV and PCBM monoadduct. The power conversion efficiency for these cells measured under monochromatic illumination (500 nm, 1 mW/cm^2) was 1.5%. From an analysis of the dependence of short-circuit current on the device thickness, for MDMO–PPV:PCBM (1:3) monoadduct active layer sandwiched between Al and ITO electrodes, a maximum power conversion efficiency of approximately 3% was extrapolated for optimized thickness of the active layer.

Note added in proof

The recent tremendous increase in the efficiency of the PPV:PCBM solar cells [12] above the limits estimated in this paper is due to an improvement of the morphology of the interpenetrating network resulting in higher carrier mobilities.

Acknowledgements

This work was carried out within the Christian Doppler Foundations dedicated laboratory for Plastic Solar Cells. Further support by the Austrian “Fonds zur Förderung der wissenschaftlichen Forschung” (Project No. P-12680-CHE) and :Forschungsförderungsfonds für die gewerbliche Wirtschaft” (Project No. 313129) are gratefully acknowledged. In addition, we want to thank the companies Aventis, Bayer and Nesté Oy for supplying us with the polymers.

References

- [1] C.W. Tang, *Appl. Phys. Lett.* 48 (1986) 183.
- [2] M. Granström, K. Petritsch, A.C. Arias, A. Lux, M.R. Andersson, R.H. Friend, *Nature* 395 (1998) 257.
- [3] G. Yu, J. Gao, J.C. Hummelen, F. Wudl, A.J. Heeger, *Science* 270 (1995) 1789.
- [4] N.S. Sariciftci, A.J. Heeger, *Photophysics, Charge Separation and Device Applications of Conjugated Polymer/Fullerene Composites*, in: H.S. Nalwa (Ed.), *Handbook of Organic Conductive Molecules and Polymers*, Wiley, Chichester, 1997, pp. 413–455.
- [5] C.J. Brabec, F. Padinger, V. Dyakonov, J.C. Hummelen, R.A.J. Janssen, N.S. Sariciftci, *Realization of large area flexible fullerene-conjugated polymer photocells: a route to plastic solar cells*, in: *Molecular Nanostructures, Proceedings of the International Winterschool on Electronic Properties of Novel Materials*, Kirchberg, 1998.
- [6] T. Ishida, H. Kobayashi, Y. Nakato, *J. Appl. Phys.* 73 (1993) 4344.
- [7] J. Shewchun, J. Dubow, C.W. Wilmsen, R. Singh, D. Burk, J.F. Wager, *J. Appl. Phys.* 50 (1979) 2832.
- [8] Y. Park, V. Choong, Y. Gao, B.R. Hsieh, C.W. Tang, *Appl. Phys. Lett.* 68 (1996) 2699.
- [9] I.D. Parker, *J. Appl. Phys.* 75 (1994) 1656.
- [10] W.R. Salaneck, S. Strafström, J.L. Bredas, *Conjugated Polymer Surfaces and Interfaces*, Cambridge University Press, Cambridge, 1996.
- [11] S. Berleb, W. Brüttinger, M. Schwörer, in: *Proceedings of ICSM 1998, Montpellier*, and references therein.
- [12] S. Shaheen, C. Brabec, F. Padinger, T. Fromherz, J.C. Hummelen, N.S. Sariciftci, submitted to *Nature*.